Silver Nanoparticle-Enriched Transdermal Patches of *Allium fistulosum* L.: A Novel Approach for Wound Healing and Inflammation Management

Jesvy Joby* [1], Dr. G.N Pramodini [2], Dr.Bonagiri Chandra Shekar [3]

[1]M.pharm Scholar, Dept. of Pharmacognosy, Nehru College of pharmacy Pampady, Thrissur, Kerala,India-680588

[2]Professor & HOD, Dept. of Pharmacognosy, Nehru College of pharmacy Pampady, Thrissur, Kerala,India-680588

[3]Principal & Professor, Dept of Pharmaceutical chemistry, Sree Dattha institute of pharmacy Sheriguda, Hyderabad-501510

Abstract: Medicinal plants continue to be a rich source of therapeutic agents, many of which form the basis of modern pharmaceuticals. *Allium fistulosum* L. (Welsh onion) is a widely consumed aromatic plant with reported pharmacological benefits including antibacterial, antioxidant, anti-inflammatory, and wound-healing activities. The present study investigated the pharmacological potential of the ethanolic extract of *Allium fistulosum* (EEAF) and its silver nanoparticles (AgNPs), with a focus on cytotoxicity, wound healing, and anti-inflammatory activity, along with the development of a transdermal drug delivery system. Cytotoxicity was evaluated on L929 mouse fibroblast cells using MTT assay, yielding an LC_{50} value of 221.767 µg/mL, suggesting low toxicity and good biocompatibility. Scratch assay demonstrated significant wound closure, with complete healing achieved within 72 hours compared to gradual healing in the control group. The protein denaturation method revealed a dose-dependent anti-inflammatory effect, with the extract showing inhibition values approaching that of Diclofenac sodium at higher concentrations (IC_{50} = 287 µg/mL for EEAF vs. 241 µg/mL for Diclofenac). Biosynthesized silver nanoparticles from EEAF exhibited a particle size of ~166 nm and a zeta potential of 47.6 mV, indicating excellent stability. SEM confirmed well-dispersed nanoparticles with uniform morphology. Incorporation of AgNPs into hydroxypropyl methylcellulose (HPMC) based transdermal patches yielded stable films with desirable physicochemical properties including good folding endurance (132 folds), 22.5% elongation at break, and no evidence of skin irritation. Overall, the findings suggest that *Allium fistulosum* and its AgNPs possess strong wound healing and anti-inflammatory potential

with excellent biocompatibility, making them promising candidates for future pharmaceutical and therapeutic applications.

(**Keywords** :*Allium fistulosum*; ethanolic extract; silver nanoparticles; cytotoxicity; wound healing; anti-inflammatory activity; transdermal patch; biocompatibility; herbal medicine; nanotechnology.)

Introduction

Plant-derived medicines have been utilized in healing practices since the beginning of human history. For millennia, natural sources have provided therapeutic agents, and a remarkable number of modern drugs have been isolated from nature, many of which were selected based on their use in traditional medicine. Historical evidence from manuscripts, monuments, and preserved herbal preparations highlights the deep connection between humans and nature in the pursuit of medicines [1]. Over time, pharmacognosy has evolved significantly, shifting its focus from the simple identification and isolation of natural compounds to exploring their pharmacological activities. Research in ethnobotany, ethnomedicine, and ethnopharmacology has become increasingly important, offering valuable insights into drug discovery and therapeutic development. Pharmacognosy continues to play a vital role in advancing novel drugs and interventions [2].

The genus Allium L., comprising more than 800 species, represents one of the largest monocotyledonous groups and includes 15 monophyletic subgenera. These species are widely distributed across the Holarctic region, ranging from dry subtropical to boreal zones [3]. Among them, *Allium fistulosum* commonly known as scallion, spring onion, Welsh onion, or Japanese bunching onion is a significant member of the Amaryllidaceae family. It is valued not only for its culinary use but also for its medicinal potential [4]. Various plant parts, including bulbs, pseudostem juice, leaves, flowers, seeds, and roots, exhibit therapeutic activities such as antibacterial, antitumor, antihypertensive, antiobesity, antioxidant, cardiovascular activation, antiplatelet aggregation, spasmolytic, and immunomodulatory effects. Its bioactive constituents include volatile oils (primarily sulfides), oleic acid, linoleic acid, allicin, pectin, and vitamin C [5].

According to the Wound Healing Society, wounds are defined as physical injuries that disrupt the skin's structural and functional integrity [6]. The wound healing process is classically divided into four overlapping stages: coagulation (hemostasis), inflammation, proliferation

(granulation), and remodeling (maturation). Typically, wounds heal within four weeks, restoring homeostasis, skin barrier, elasticity, and physiological function [7].

Silver nanoparticles (Ag-NPs), defined as natural, incidental, or engineered particles with sizes predominantly in the 1–100 nm range, have gained attention for their diverse biomedical and industrial uses [8]. Due to their unique optical, electrical, and thermal properties combined with biological effects—Ag-NPs are increasingly applied in antibacterial, antifungal, antiviral, anti-inflammatory, anticancer, and anti-angiogenic therapies [9].

Among modern drug delivery approaches, transdermal patches have become a highly researched system due to their ability to deliver medications effectively while improving compliance and minimizing systemic side effects [10].

Methodology

Plant Material Collection and Authentication

Leaves of *Allium fistulosum* L. were collected on 27 January 2025 from the Thrissur vegetable market, Kerala. The species was authenticated by Dr. Ranjusha A. P., Head of Botany, N.S.S. College, Ottapalam. The leaves were separated, washed, shade-dried for 25–30 days, powdered using a grinder, and stored in airtight containers for further use.

Preparation of Plant Powder

The whole plant was thoroughly washed and shade-dried for 25–30 days, ground to a coarse powder, and stored in an airtight container. Extraction is a crucial step in phytochemical studies, where suitable solvents are used to separate bioactive constituents.

Preparation of Extract

Using Soxhlet extraction, 25 g of the dried powder was extracted with ethanol (a polar solvent) at 60–70°C for 18 hours until the siphon tube solution became colorless. The concentrated extract was obtained using a rotary evaporator and stored as a semisolid residue in a desiccator [11].

In Vitro Pharmacological Screening

In Vitro Cytotoxic Effect Determination by MTT Assay

L929 (mouse fibroblast) cells were obtained from the National Centre for Cell Sciences (NCCS), Pune, India, and cultured in Dulbecco's Modified Eagle's Medium (DMEM, Sigma Aldrich, USA). The cells were maintained in 25 cm^2 tissue culture flasks with DMEM

supplemented with 10% fetal bovine serum (FBS), L-glutamine, sodium bicarbonate (Merck, Germany), and an antibiotic mixture containing penicillin (100 U/ml), streptomycin (100 µg/ml), and amphotericin B (2.5 µg/ml). Cultures were incubated at 37°C in a humidified atmosphere with 5% CO_2 using an incubator (NBS Eppendorf, Germany). The MTT assay was employed to evaluate cell viability following direct microscopic observation with an inverted phase-contrast microscope.

Cell Seeding in 96-Well Plates

A confluent monolayer culture (2 days old) was trypsinized, and the cells were resuspended in 10% growth medium. An aliquot of 100 µl cell suspension (5×10^3 cells/well) was seeded into a 96-well culture plate and incubated at 37°C in a humidified 5% CO_2 incubator.

Preparation of Compound Stock

One milligram of the test sample was dissolved in 1 ml of 0.1% DMSO using a cyclomixer. The solution was filtered through a 0.22 µm Millipore syringe filter to maintain sterility.

Cytotoxicity Evaluation

After 24 h of incubation, the culture medium was removed, and cells were treated with freshly prepared test solutions at concentrations of 100, 50, 25, 12.5, and 6.25 µg/ml in DMEM. Each concentration was tested in triplicate, and untreated cells served as the control. The plates were incubated at 37°C in a humidified 5% CO_2 environment.

Microscopic Observation of Cytotoxicity

After 48 h of treatment, the entire plate was examined under an inverted phase-contrast microscope (Olympus CKX41 with Optika Pro5 CCD camera). Morphological changes such as cell rounding, shrinkage, granulation, or cytoplasmic vacuolization were considered as indicators of cytotoxic effects.

MTT Assay for Cytotoxicity

MTT solution was prepared by dissolving 15 mg of MTT (Sigma, M-5655) in 3 ml of PBS, followed by filter sterilization. After 48 h of incubation with test samples, the medium was discarded, and 30 µl of MTT solution was added to each well. The plates were gently agitated and incubated at 37°C in a humidified 5% CO_2 incubator for 4 h. After incubation, the

supernatant was removed, and 100 µl of solubilization solution (dimethyl sulfoxide, DMSO; Sigma Aldrich, USA) was added to dissolve the formazan crystals by gentle pipetting. The absorbance was measured at 540 nm using a microplate reader [12, 13].

The percentage of growth inhibition was calculated using the formula

$$\% \text{ of viability} = \frac{\text{Mean OD of samples} \times 100}{\text{Mean OD of control group}}$$

In Vitro Wound Healing Activity by Scratch Assay

L929 (mouse fibroblast) cells were procured from the National Centre for Cell Sciences (NCCS), Pune, India, and cultured in Dulbecco's Modified Eagle's Medium (DMEM; Gibco, Invitrogen). The cells were maintained in 25 cm^2 tissue culture flasks with DMEM supplemented with 10% fetal bovine serum (FBS), L-glutamine, sodium bicarbonate, and an antibiotic cocktail containing penicillin (100 U/ml), streptomycin (100 µg/ml), and amphotericin B (2.5 µg/ml). Cultures were incubated at 37°C in a humidified atmosphere of 5% CO_2 using an NBS Eppendorf incubator.

Sample Preparation

One milligram of the test sample was dissolved in 1 ml of 0.1% DMSO with the aid of a cyclomixer. The prepared solution was filtered through a 0.22 µm Millipore syringe filter to ensure sterility.

Procedure

Exponentially growing cells were trypsinized and seeded into 12-well plates at a density of 2 × 10^5 cells per well and incubated for 24 h until ~90% confluence was achieved. A sterile 1 ml pipette tip was used to create linear scratch wounds across pre-marked areas. Cell debris generated from the scratches was removed, and the monolayer was rinsed three times with PBS. Cells were then treated with the sample (12.5 µg/ml) and incubated for 0, 24, 48, and 72 h. Images of wound areas were captured at the intersections of the scratch lines and pre-marked regions using an inverted microscope (Olympus CKX41, 4× magnification). Wound closure was quantified by measuring the wound area with MRI-Image analysis software [14].

In Vitro Anti-Inflammatory Activity by Protein Denaturation Method

Preparation of 1% Egg Albumin Solution

To prepare a 1% egg albumin solution, a fresh hen's egg was cracked carefully, and 1 mL of the translucent portion (egg white/albumin) was transferred into 100 mL of distilled water (w/v). The mixture was stirred thoroughly to obtain a uniform solution. Cold water was used for preparation, as heating water to boiling point may cause coagulation of the albumin.

Egg Albumin Assay

The in vitro anti-inflammatory activity of crude plant extracts was evaluated based on their ability to inhibit egg albumin (protein) denaturation.

- The reaction mixture (5 mL total volume) consisted of 0.2 mL of 1–2% egg albumin solution (from fresh egg or commercial powder), 2 mL of test extract or standard drug (Diclofenac sodium) at different concentrations, and 2.8 mL of phosphate-buffered saline (PBS, pH 7.4).
- For the control, 5 mL was prepared by mixing 2 mL of triple-distilled water, 0.2 mL of 1–2% egg albumin solution, and 2.8 mL of PBS.
- All mixtures were incubated at 37 ± 2°C for 30 minutes, followed by heating in a water bath at 70 ± 2°C for 15 minutes.
- After cooling, absorbance was measured at 280 nm using a UV–Vis spectrophotometer, with triple-distilled water as the blank.
- The percentage inhibition of protein denaturation was calculated using the following formula:

$$\% \text{ Inhibition} = \frac{A_{control} - A_{sample}}{A_{control}} \times 100$$

The concentration of plant extract or positive control required to achieve 50% inhibition (IC_{50}) was determined by plotting percentage inhibition against concentration [15].

Biosynthesis of Silver Nanoparticles from Leaves of *Allium fistulosum* L

Five grams of finely powdered leaves were mixed with 100 mL of deionized water and boiled for 5 minutes, followed by decantation. The resulting suspension was centrifuged at 5,000 rpm for 15 minutes at 40°C using fresh deionized water. The extract volume was adjusted with deionized water to the required level and then filtered through Whatman No. 1 filter paper. For

the reduction of Ag^+ ions, 10 mL of the extract was mixed with 90 mL of 1 mM aqueous $AgNO_3$ solution and incubated in the dark at room temperature for 24 hours. The formed silver nanoparticles were separated by centrifugation at 10,000 rpm for 20 minutes, washed three times with deionized water, and stored as lyophilized powder [16].

Evaluation of Silver Nano Particles

The behavior of silver nanoparticles is influenced by factors like size, shape, stability, and distribution. Therefore the nanoparticles are characterized by the following evaluation parameters:

- Measurement of Zeta potential (ZP)
- Measurement of particle size (PS)
- SEM analysis

a. Measurement of Zeta Potential (ZP)

The surface charge of the optimized nanoparticles was determined using a Zetasizer Nano ZS90. The sample was diluted with water to a final volume of 10 mL, and 5 mL of this diluted sample was placed in a cuvette for ZP measurement [17].

b. Measurement of Particle Size (PS)

The particle size was measured using a particle size analyzer based on dynamic light scattering (DLS). Since particles suspended in liquid undergo Brownian motion, the rate of movement varies with size—smaller particles move faster than larger ones. Light scattering patterns were recorded and compared to calculate the average particle size and size distribution [17].

c. SEM Analysis

SEM was employed to study the morphological features of silver nanoparticles. Lyophilized nanoparticles were mounted on specimen stubs using double-sided adhesive tape and coated with gold using a sputter coater (BAL-TEC SCD-005). The samples were observed under a Philips XL-30 SEM at an accelerating voltage of 12–16 kV with a 45° tilt angle [18].

Preparation of Silver Nano Particle Incorporated Transdermal Patch of *Allium fistulosum* L., Ethanol Extract

 A solvent mixture of chloroform (7.5 mL) and ethanol (7.5 mL) in a 1:1 ratio was prepared.

 Hydroxypropyl methylcellulose (HPMC, 180 mg) was dissolved in the solvent under stirring.

 Glycerin (0.1 mL) and PEG 400 (0.1 mL) were added.

 Fifteen milligrams of silver nanoparticles from *Allium fistulosum* extract were dissolved in a few drops of ethanol, incorporated into the above mixture, and stirred magnetically for 30 minutes.

 A few drops of menthol were added.

 The final solution was cast into a Petri dish and left overnight to dry [19].

Evaluation of Transdermal Patches

Transdermal patches are designed to enhance therapeutic efficacy and patient compliance by ensuring controlled drug release. Hence, various evaluation studies were performed:

a. Organoleptic Properties: Physical characteristics such as appearance, color, smoothness, flexibility, and clarity were examined visually.

b. Thickness: Film thickness was measured at multiple points using a traveling microscope, screw gauge, micrometer, or dial gauge.

c. Uniformity of Weight: Ten patches were randomly selected, weighed individually, and the average weight was calculated. Deviations from the average were assessed.

d. Moisture Content: Films were weighed and placed in a desiccator containing calcium chloride at room temperature for 24 hours. They were reweighed at fixed intervals until a constant weight was achieved. The percentage of moisture content was then calculated.

e. Folding Endurance: Films were folded repeatedly at the same site until they broke. The number of folds tolerated without breaking indicated the folding endurance.

f. Percentage Elongation Break Test: Elongation at break was determined using the formula:

$$\% \text{ Elongation} = \frac{L_1 - L_2}{L_2} \times 100$$

Where L_1 = final length of strip before breaking and L_2 = initial length of strip.

g. Skin Irritation Test: The prepared *Allium fistulosum* patch was applied to the skin for 20–30 minutes. After removal, the treated area was visually examined for signs of irritation [20, 21].

Result and Discussion

In Vitro Acute Toxicity Studies

Table 1: In vitro acute toxicity study of EEAF

Sample Concentration (µg/mL)	OD value I	OD value II	OD value III	Average OD	Percentage Viability
Control	0.9423	0.9384	0.9476	0.9428	100.00
Sample Code: Samples(EEAF)					
6.25	0.9256	0.9142	0.9117	0.9172	97.28
12.5	0.8654	0.8528	0.85551	0.8579	91.00
25	0.819	0.8002	0.8031	0.8074	85.64
50	0.7646	0.7528	0.7551	0.7575	80.35
100	0.7135	0.7225	0.7236	0.7199	76.35

LC50 Value (Sample): 221.767 µg/mL (Calculated using ED50 PLUS V1.0 Software)

Graph 1: percentage of viability

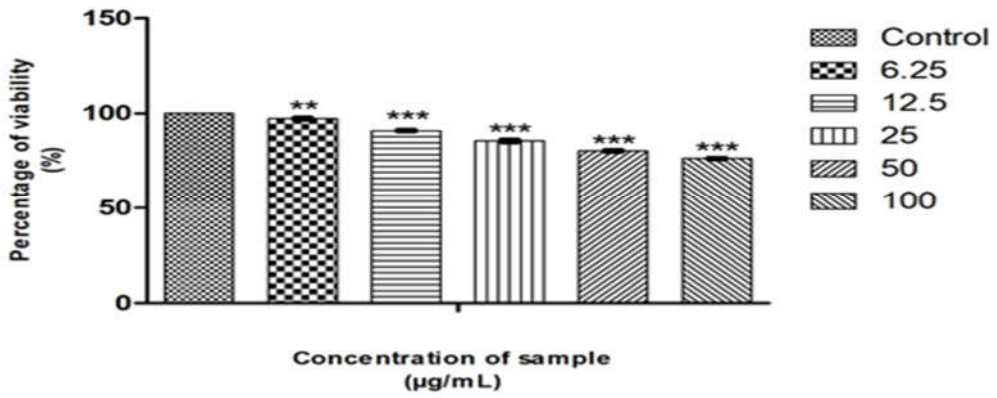

The test sample exhibited a dose-dependent reduction in cell viability; however, more than 75% of cells remained viable even at the maximum tested concentration (100 µg/mL), suggesting minimal cytotoxicity. The LC_{50} value, calculated as 221.767 µg/mL, further indicates that only a relatively high concentration can cause significant effects on cell viability. These findings demonstrate that the sample possesses low toxicity and good biocompatibility, making it a promising and safe candidate for future biological or pharmaceutical applications.

Fig 1: EEAF 6.25µg/ml

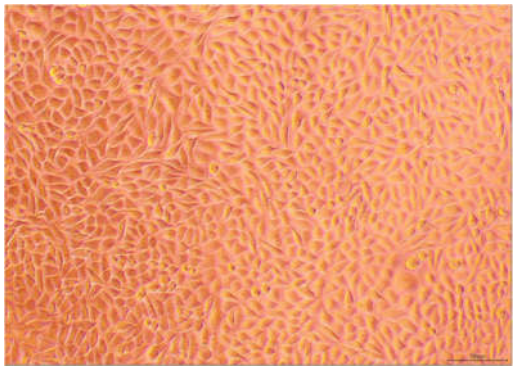

Fig 2: EEAF 12.5µg/ml

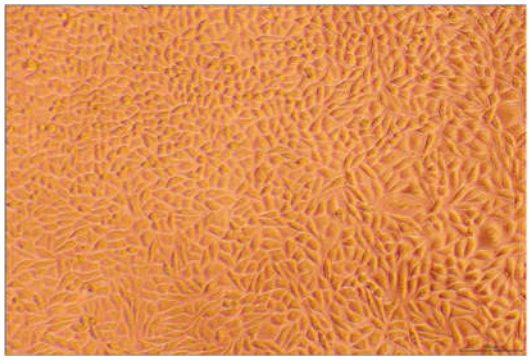

Fig 3: EEAF 25µg/ml

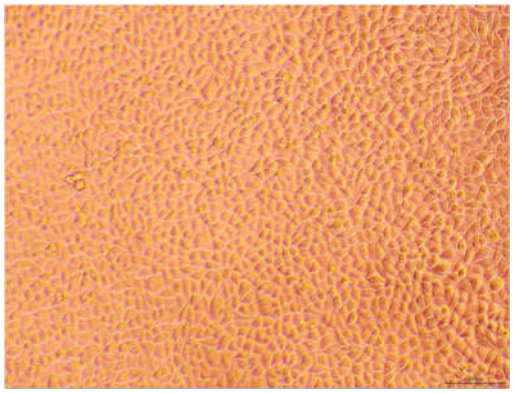

Fig 4: EEAF 50µg/ml

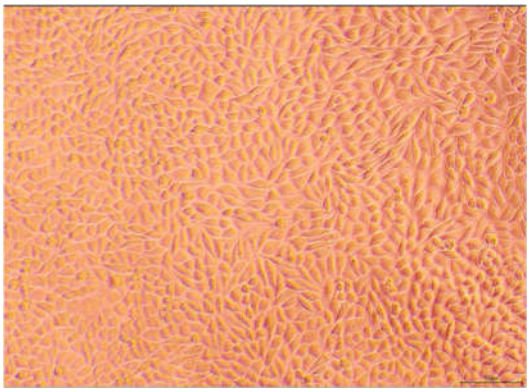

Fig 5: EEAF 100µg/ml

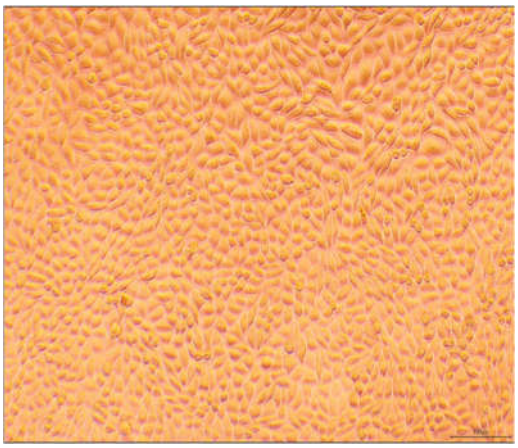

Fig 6: Control

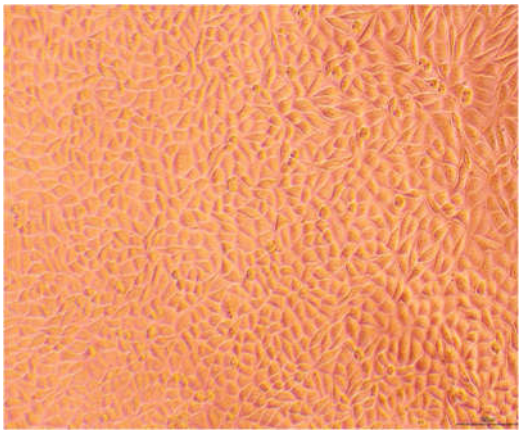

IN VITRO WOUND HEALING ACTIVITY

Table 2: In vitro wound healing of EEAF

Time Interval (hrs)	Scratch area (px)
CONTROL 0 HR	1460210
SAMPLE 0 HR	1459032
CONTROL 24 HR	1271862
SAMPLE 24 HR	843195
CONTROL 48 HR	707538
SAMPLE 48 HR	242421
CONTROL 72 HR	533349
SAMPLR 72 HR	0

Graph 2: Wound area

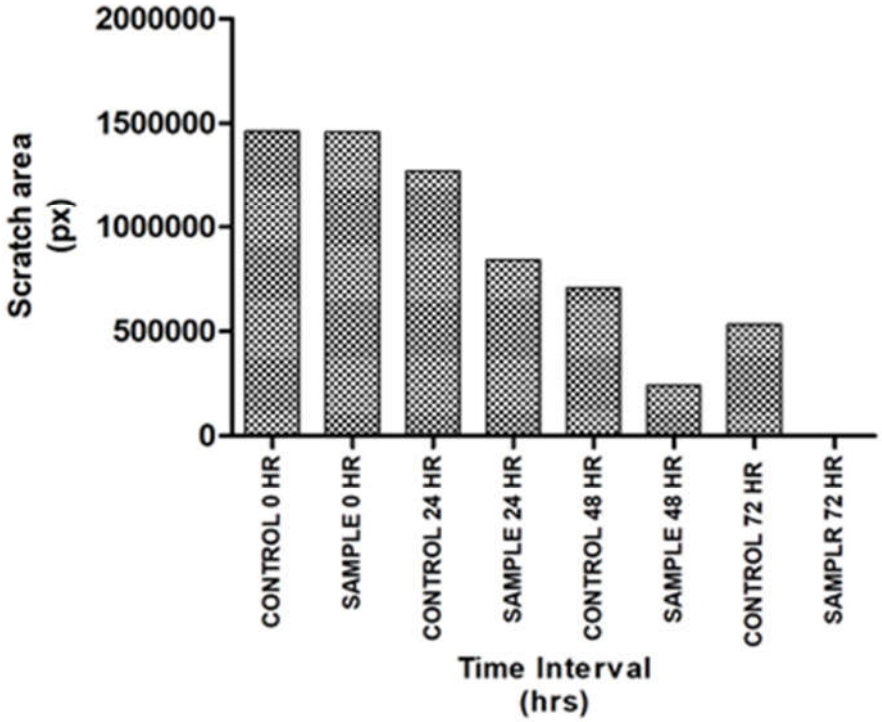

Fig 7: Control at 0 hr.

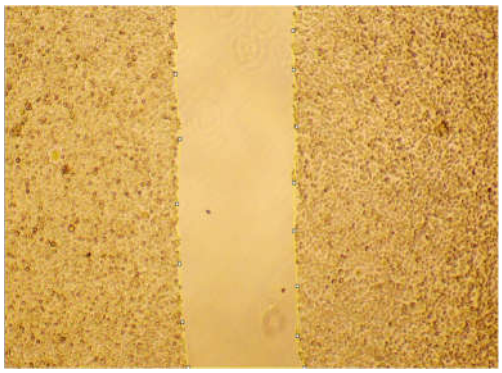

Fig 8: EEAF at 0 hr.

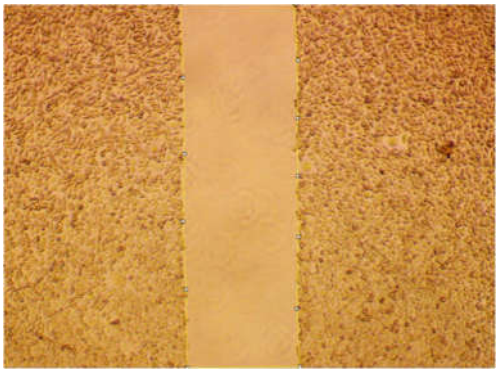

Fig 9: Control at 24hr

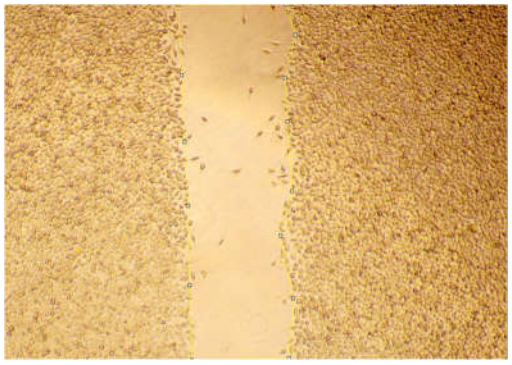

Fig 10: EEAF at 24 hr.

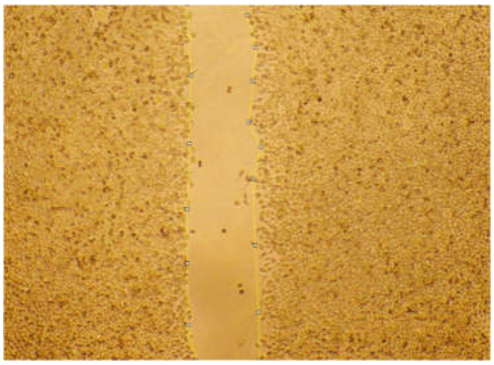

Fig 11: Control at 48 hr.

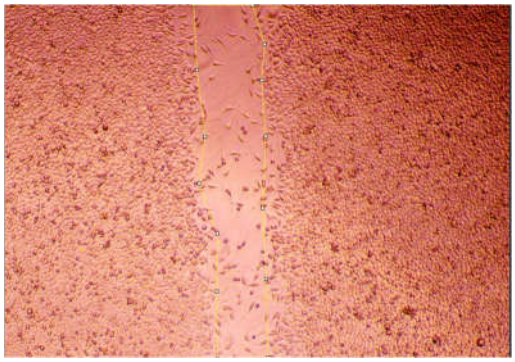

Fig 12: EEAF at 48 hr.

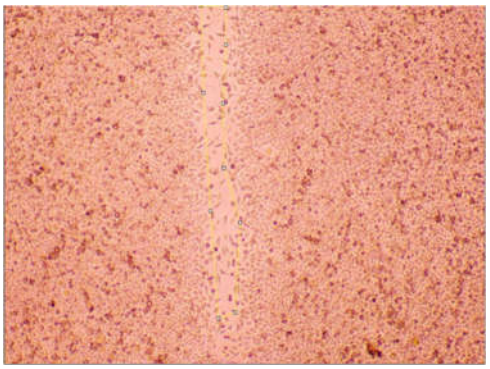

Fig 13: Control at 72 hr.

Fig 14: EEAF at 72 hr.

The findings indicate that the sample exerts a pronounced wound healing effect, markedly enhancing the rate of closure when compared to the control group. While the control group displayed a slow and progressive reduction in wound area, the treated group showed rapid recovery, achieving complete closure within 72 hours. These results suggest that the sample holds significant wound healing potential and may serve as a promising candidate for further exploration in therapeutic wound management.

In Vitro Anti Inflammatory Activity

The anti-inflammatory activity of *Allium fistulosum* was carried out across varying concentrations.

Table 3: In vitro Anti-inflammatory of EEAF

Concentration	Absorbance (Standard Diclofenac)	Percentage inhibition	Absorbance (Plant extract)	Percentage inhibition
100	0.52±0.04	36%	0.60±0.02	26%
200	0.46±0.02	43%	0.51±0.03	37%
300	0.32±0.05	60%	0.39±0.05	52%
400	0.24±0.03	70%	0.29±0.04	64%
500	0.19±0.02	76%	0.23±0.05	71%

IC50 VALUES

Standard Diclofenac -241 µg/mL

Plant Extract - 287 µg/mL

Graph 3: Anti-inflammatory activity of EEAF

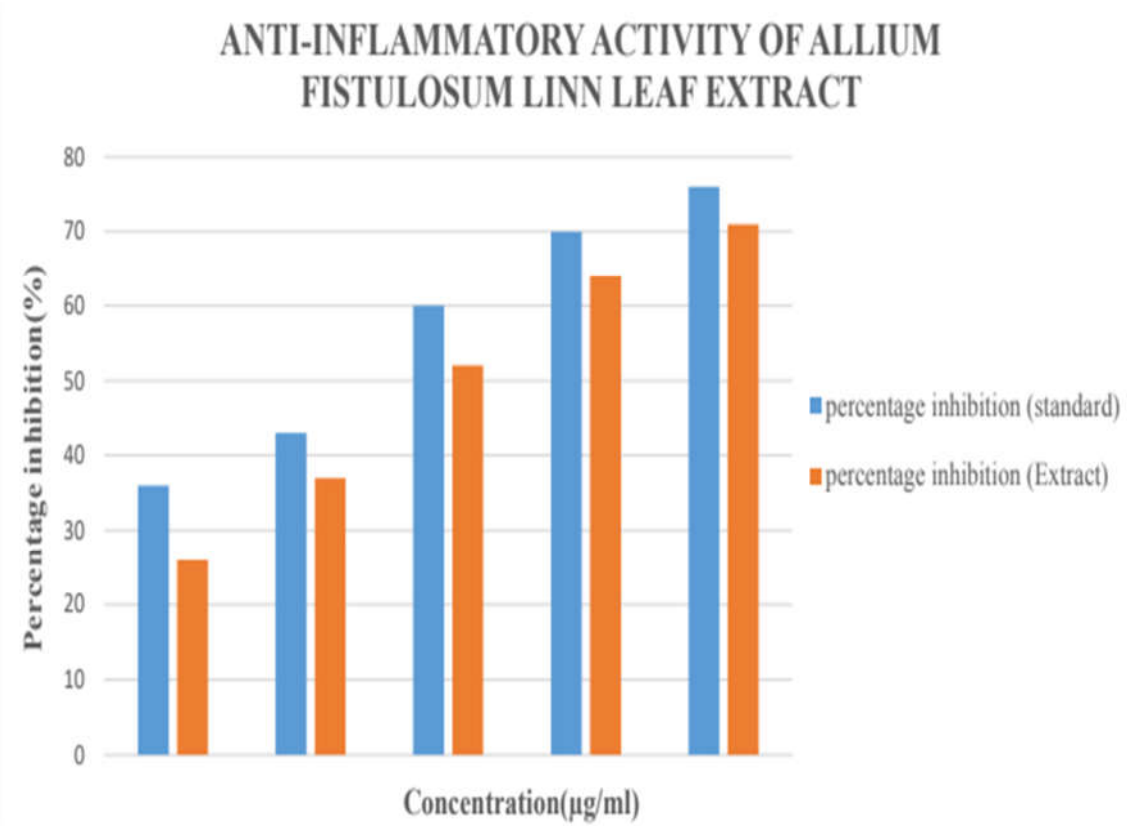

Both the standard and the test sample showed a distinct dose-dependent rise in percentage inhibition, demonstrating enhanced inhibitory activity with increasing concentrations. At every concentration tested, the standard produced greater inhibition than the sample. However, the difference between them narrowed at higher doses, where the test sample exhibited inhibition values comparable to the standard. This indicates that the test sample has considerable inhibitory potential, particularly at elevated concentrations.

Biosynthesis of Silver Nanoparticles from EEAF

Silver nano particles were synthesized from the ethanolic exract of *Allium fistulosum* linn

Fig 15: Silver nanoparticles from EEAF

Fig 16: Powder of Silver Nano particles

Evaluation of Silver Nano Particles

Particle Size

Particle size is measured in litesizer 500 in a temperature 25.0 °C with a solvent using water.

The particle hydrodynamic diameter is 166.59nm

Graph 4: Particle size of Silver Nano particle

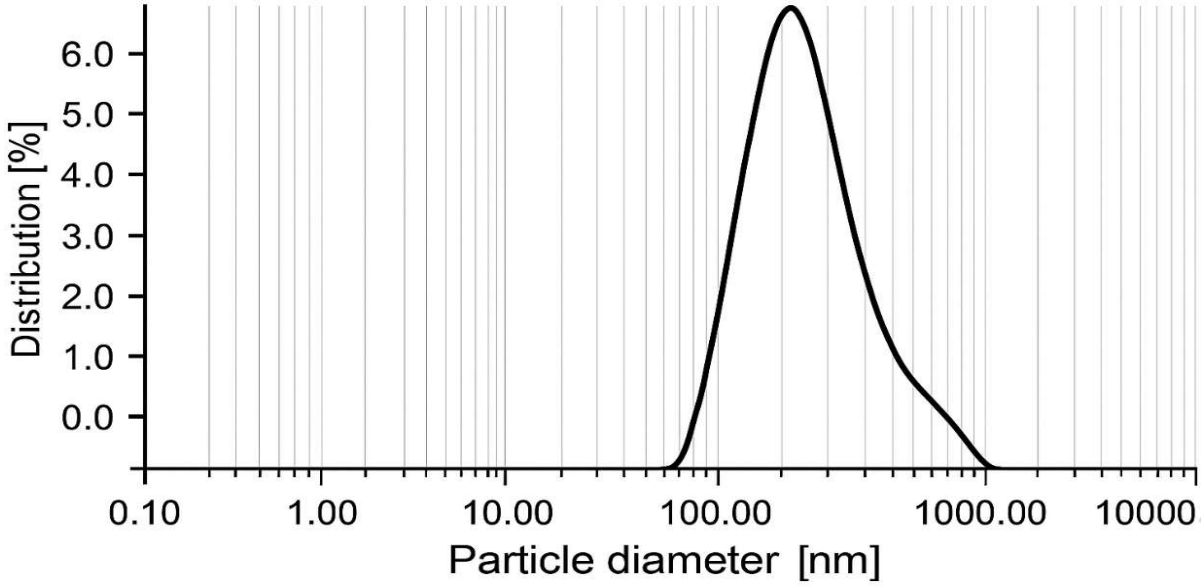

A nanoparticle size of 166 nm falls within the intermediate range (1–1000 nm), making it appropriate for diverse applications, especially in drug delivery and diagnostic fields. Particles of this dimension provide an optimal balance between surface area and volume, allowing effective functionalization and interaction with biological systems. Factors such as stability, biocompatibility, and targeting ability remain critical for their potential use.

Zeta Potential

Zeta potential serves as an important parameter for assessing the stability of colloidal systems, including nanoparticles, as it reflects the degree of electrostatic repulsion or attraction among suspended particles [68]. A measured zeta potential of –47.6 mV indicates a highly stable colloidal dispersion, where particles remain well-dispersed with minimal risk of aggregation. The strong negative surface charge generates sufficient repulsion to prevent particle clustering or sedimentation. This property is particularly valuable in applications such as drug delivery, where surface charge plays a critical role in influencing cellular interactions and uptake.

Graph 5: Zeta potential of Silver Nano particle

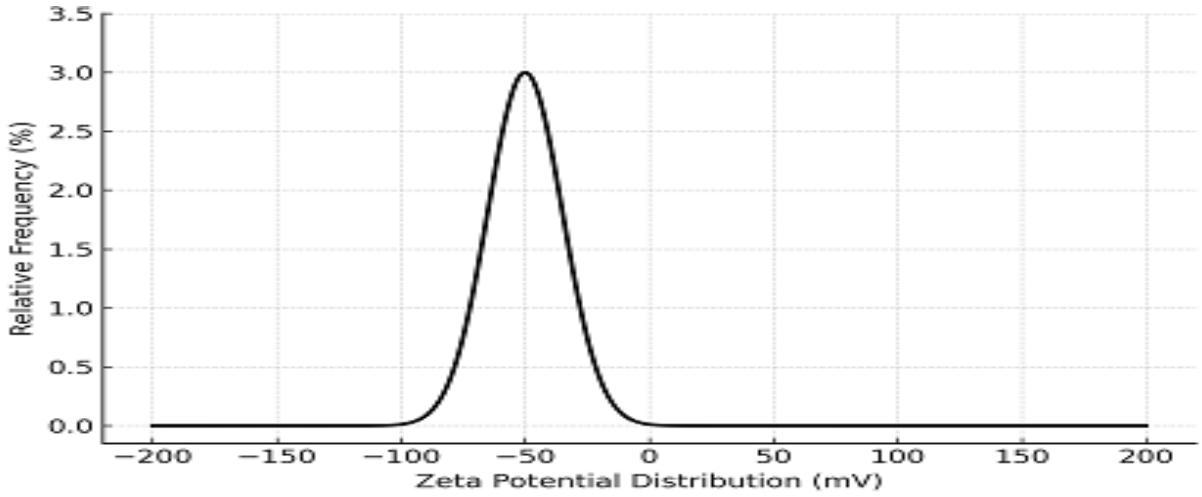

Scanning Electron Microscopy (SEM)

Scanning Electron Microscopy (SEM) is widely used to examine particle morphology, size, and shape, whereas zeta potential analysis provides insights into surface charge and colloidal stability. The graph shows a distinct peak near –50 mV, suggesting that the majority of particles possess a strong negative charge, which helps maintain stability by reducing aggregation. SEM serves as a complementary technique by visually verifying particle distribution. In this context, the negative zeta potential indicates that SEM images would likely display well-dispersed and stable particles, correlating electrostatic stability with morphological characteristics**.**

Fig 17: SEM analysis of Silver Nano particle

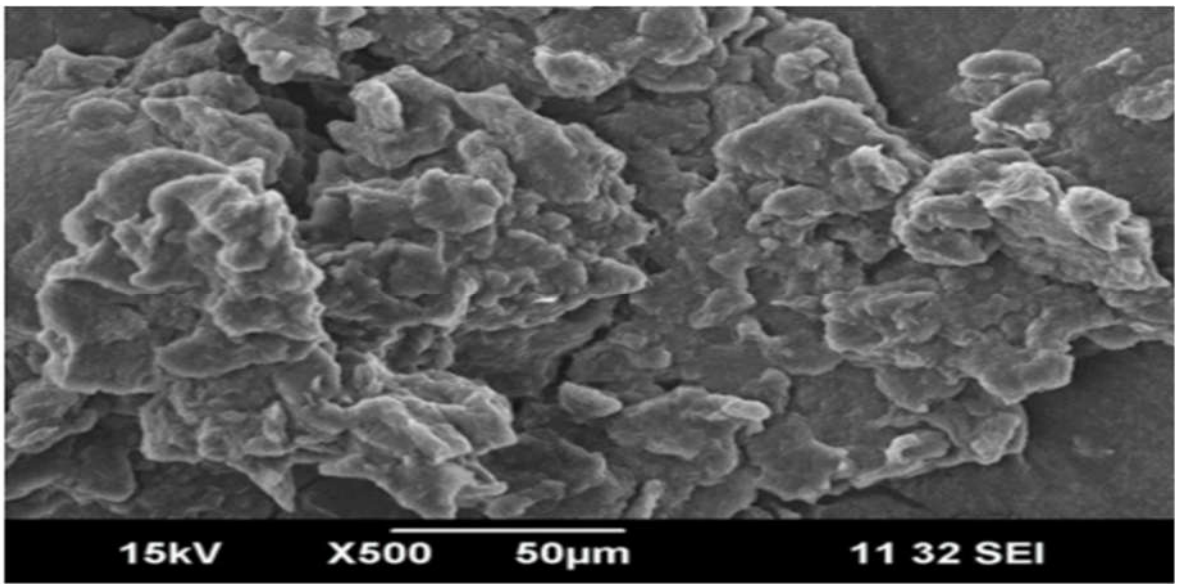

PREPARATION OF SILVER NANO PARTICLE INCOPORATED TRANSDERMAL PATCH

By using silver Nano particle, transdermal patch is produced

Fig 18: Transdermal patch

Evaluation Test for Transdermal Patches

Organoleptic Characteristics

The physical appearance of developed patch was evaluated by using a naked-eye examination for its appearance, colour, clarity, flexibility, and smoothness.

Table 4: Organoleptic characteristics

Sl. No	Physical Appearance	Observation
1	Appearance	Jellified Preparation
2	Colour	Yellowish green
3	Clarity	Opaque
4	Flexibility	Yes
5	Smoothness	Good

Uniformity of Weight

Table 5: Uniformity of weight

Wt Of Individual Patch (g)	Average Weight Of Patch (g)
0.254	0.2525
0.250	
0.252	
0.255	
0.253	
0.251	

Folding Endurance

Folding endurance was determined by repeatedly folding the film at the same point until it broke. The film withstood 132 folds at the same spot before breaking, indicating its folding endurance value.

Percentage Elongation Break Test

Initial length of patch (L2) = 4.0 cm

Final length of patch at break (L1) = 4.9 cm

Therefore, percentage elongation = 22.5 %

Skin Irritation Test

The skin irritation study of *Allium fistulosum* L. patches revealed no signs of itchiness, rash, or burning sensations.

Conclusion

The present study highlights the therapeutic potential of *Allium fistulosum* L., an aromatic and medicinal plant, through its ethanolic extract (EEAF) and biosynthesized silver nanoparticles (AgNPs). The in vitro pharmacological evaluations demonstrated that EEAF possesses significant biological activity with high safety margins. Cytotoxicity analysis using the MTT assay on L929 fibroblast cells revealed minimal toxicity, with more than 75% cell viability

maintained even at the highest concentration tested and an LC_{50} value of 221.767 µg/mL, confirming its biocompatibility.

Wound healing assessment through the scratch assay indicated a remarkable enhancement in fibroblast migration and wound closure, with complete healing observed within 72 hours in the treated group, compared to the slower recovery in the control. This strongly suggests that the bioactive compounds in *Allium fistulosum* effectively stimulate cellular proliferation and tissue regeneration.

The anti-inflammatory potential of EEAF was established using the protein denaturation assay, where the extract showed dose-dependent inhibition comparable to diclofenac sodium, with an IC_{50} of 287 µg/mL. Although slightly less potent than the standard, the extract demonstrated promising inhibitory activity, supporting its role as a natural anti-inflammatory agent.

Green synthesis of silver nanoparticles from EEAF further enhanced its therapeutic potential. The AgNPs exhibited an average particle size of 166 nm and a zeta potential of –47.6 mV, indicating strong stability and resistance to aggregation. SEM analysis confirmed well-dispersed nanoparticles with uniform morphology. These properties make the nanoparticles highly suitable for biomedical applications, particularly drug delivery.

Incorporation of AgNPs into hydroxypropyl methylcellulose (HPMC)-based transdermal patches yielded stable and flexible films with desirable physicochemical properties, including a folding endurance of 132 folds, elongation at break of 22.5%, and no signs of irritation in skin studies. These findings indicate that the formulated patches are safe for topical application and capable of delivering therapeutic agents effectively.

Overall, this study establishes *Allium fistulosum* and its silver nanoparticle formulations as promising candidates for wound healing and anti-inflammatory therapies. The combination of low cytotoxicity, strong bioactivity, and effective delivery through transdermal patches provides a foundation for future development into clinically relevant pharmaceutical products. Further in vivo investigations, mechanistic studies, and clinical trials are warranted to validate their therapeutic efficacy and safety in humans.

Acknowledgment

I would like to thank Nehru College of pharmacy for the support and lab facilities.

Reference

1. Hossain Cm, Gera M, Ali Ka. Current Status and Challenges of Herbal Drug Development and Regulatory Aspect: A Global Perspective. Asian Journal of Pharmaceutical and ClinicalResearch. 2022 Dec 7; 31–41.
2. Petrovska BB. Historical review of medicinal plants′ usage. Pharmacognosy Reviews. 2012; 6(11):1.
3. Maragheh FP, Janus D, Senderowicz M, Haliloglu K, Kolano B. Karyotype analysis of eight cultivated Allium species. Journal of applied genetics. 2019 Feb 7; 60:1-1.
4. Kim SH, Yoon JB, Han J, Seo YA, Kang BH, Lee J, Ochar K. Green onion (Allium fistulosum): an aromatic vegetable crop esteemed for food, nutritional and therapeutic significance. Foods. 2023 Dec 16; 12(24):4503.
5. Padula G, Xia X, Hołubowicz R. Welsh onion (Allium fistulosum L.) seed physiology, breeding, production and trade. Plants. 2022 Jan 27; 11(3):343.
6. Nagori BP, Solanki R. Role of medicinal plants in wound healing. Research Journal of Medicinal Plant. 2011 Apr 1; 5(4):392-405.
7. Shedoeva A, Leavesley D, Upton Z, Fan C. Wound healing and the use of medicinal plants. Evidence-Based Complementary and Alternative Medicine. 2019; 2019(1):2684108.
8. Mathur P, Jha S, Ramteke S, Jain NK. Pharmaceutical aspects of silver nanoparticles. Artificial cells, nanomedicine, and biotechnology. 2018 Oct 31; 46(sup1):115-26.
9. Zhang XF, Liu ZG, Shen W, Gurunathan S. Silver nanoparticles: synthesis, characterization, properties, applications, and therapeutic approaches. International journal of molecular sciences. 2016 Sep 13; 17(9):1534.
10. Alam MI, Alam N, Singh V, Alam MS, Ali MS, Anwer T, Safhi MM. Type, preparation and evaluation of transdermal patch: a review. World journal of pharmacy and pharmaceutical sciences. 2013 May 21; 2(4):2199-233.
11. Monika N, and Sakthi A. Evaluation of invitro anticancer activity of bulb extracts of allium fistulosum l. against hepatocellular carcinoma cell line (hep g2). World journal of pharmacy and pharmaceutical sciences. 2018 Apr 30; Volume 7(Issue 5):1678–99.
12. Mosmann T. Rapid colorimetric assay for cellular growth and survival: Application to proliferation and cytotoxicity assays. Journal of Immunological Methods. 1983 Dec; 65(1–2):55–63.

13. Ramachandran R, Saraswathy M. Postconditioning with metformin attenuates apoptotic events in cardiomyoblasts associated with ischemic reperfusion injury.Cardiovascular Therapeutics. 2017 Dec;35(6):e12279
14. Das SK, Chakraborty S, Rajabalaya R, Mazumder B. Zeta potential measurements and analysis for biomedical nanotechnology. In: Analytical Techniques for Biomedical Nanotechnology 2023 Jul 1 (pp. 17-1). Bristol, UK: IOP Publishing.
15. HDT M. In vitro anti-inflammatory egg albumin denaturation assay: An enhanced approach. Journal of Natural & Ayurvedic Medicine. 2023; 7(3):1-6.
16. Banerjee J, Narendhirakannan RT. Biosynthesis of silver nanoparticles from Syzygium cumini (L.) seed extract and evaluation of their in vitro antioxidant activities. Dig J Nanomater Biostruct. 2011 Jul 1; 6(3):961-8.
17. Patel J., Patel R., Khambholja K., Patel N. An overview of phytosomes as an advanced herbal drug delivery system. Asian Journal of Pharmaceutical Sciences. 2009 Apr; 4(6):363-371.
18. Forough M, Farhadi K. Biological and green synthesis of silver nanoparticles. Turkish J. Eng. Env. Sci. 2010 Dec 1; 34(4):281-7.
19. Patel RP, Patel G, Baria A. Formulation and evaluation of transdermal patch of aceclofenac.International Journal of Drug Delivery. 2009 Jul 5; 1(1):41–51.
20. Alam MI, Alam N, Singh V, Alam MS, Ali MS, Anwer T, Safhi MM. Type, preparation and evaluation of transdermal patch: a review. World journal of pharmacy and pharmaceutical sciences. 2013 May 21; 2(4):2199-233.
21. Prajapati ST, Patel CG, Patel CN. Formulation and evaluation of transdermal patch of repaglinide. International Scholarly research notices. 2011; 2011(1):651909.